Superior School of Technology and Experimental Sciences

Department of Physical and Analytical Chemistry

STUDY OF THE HEATING CAPACITY ENHANCEMENT OF SOLAR SALTS BY THE ADDITION OF SILICA NANOPARTICLES

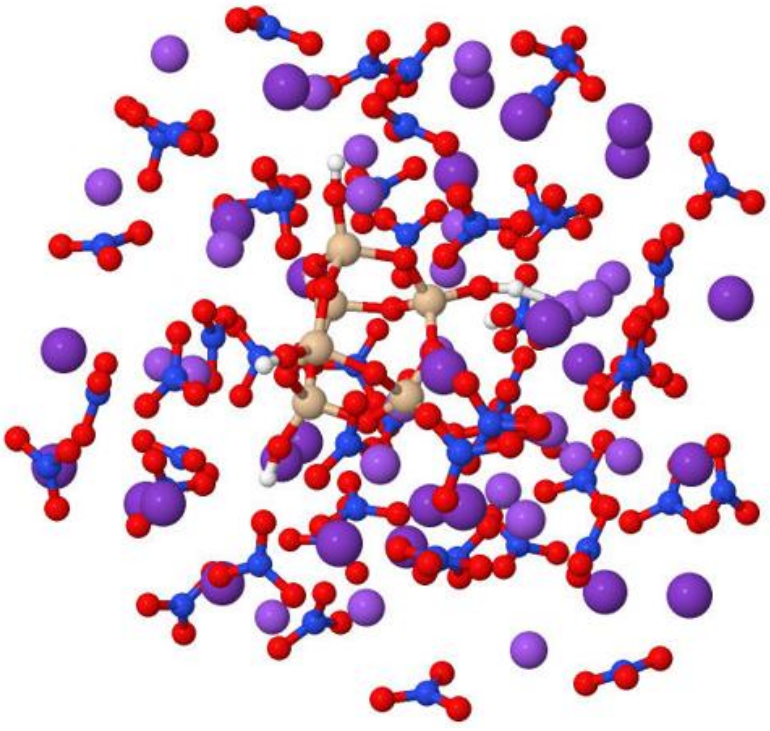

Author: Marc Sánchez Quesada

Supervisor: Sergio Martí Forés

QU0943- Final Degree Project

2019/2020

INDEX

1. ACKNOWLEDGEMENTS

First of all, I would like to thank Sergio, who has been my tutor throughout this process. From the beginning he allowed me to choose a topic that was of interest to me and always gave me freedom to decide the path this work would take. He has known how to explain very complicated concepts to me in a very simple way, making my work much easier throughout this journey. It has been a pleasure to work with him.

I would also like to thank Rosa Mondragon and her research team who started this project, providing us with the experimental spectra of solar salts, nanoparticles and nanofluid, as well as all the information on the topic in question with two papers that will be cited later.

Finally, I would also like to thank Santiago Rodriguez Pastor, who helped me when I was blocked and did not know how to advance, and without which this work would probably not have reached this point.

2. INTRODUCTION

Over the last years, solar thermal salts have been studied as natural solution for storage and heat transfer in Concentrating Solar Power Plants (CSP). This new kind of renewable energy has become one of the alternatives of fossil fuels. The CSP plants transform the solar energy into electricity by the Thermal Energy Storage (TES) properties of this kind of material, which allows to store large amounts of heat. These types of salts provide a high thermal stability, low material costs, high density of the salt fluid, high heat storage capacity, non-flammability and low vapor pressure. In addition, compared with organic salts these inorganic salts present a higher melting point. [1]

A large quantity of inorganic salts have been used as solar salt systems in CSP plants, mixtures of carbonates (Li_2CO_3 and K_2CO_3), mixtures of chlorides ($BaCl_2$, NaCl and $CaCl_2$) and finally, the most commonly used, a mixture of sodium and potassium nitrates ($NaNO_3$:KNO_3). [2]

An interest in the enhancement of the heat capacity in solar salts with the addition of nanoparticles has been grown in the last years. In 2011, Shin and Banerjee [3] reported an unusual specific heat enhancement when silica nanoparticles were added to carbonate and chloride salts mixtures. These results were obtained when the solar salts were doped with 1-2 %wt of nanoparticles. The increase of the specific heat of the nanofluid seems to be against the mixture rule, which states that the specific heat of a nanofluid should decrease if the added nanoparticles have a lower specific heat than the fluid itself. This theory applies to molecular liquids, such as alcohols, thermal oils, ethylene glycol or water.

A large number of proposals for this increase in specific heat have been put forward, such as the formation of a thermal resistance due to an electrostatic force between the nanoparticles and the liquid solar salt, the formation of a semi-solid barrier on the surface of the liquid with thermal properties greater than the liquid itself or the introduction of the nanoparticles into the solar salt from an oxygen-nitrogen bond, generating a nanofluid with calorific properties greater than the liquid solar salt itself.

It has been shown that the conditions in which this nanofluid is prepared are very important in obtaining this increase in heat capacity. All the authors agree that the enhancement in heating capacity depends on the available specific surface area of the nanoparticles and on the nanoparticle-salt interaction, which occurs at the key stage corresponding to the formation of the nanofluid. The maximum increase in heating capacity has been recorded at 1-2 %wt in nanoparticles.

---

[1] Nicole, P.; Thomas, B.; Claudia, M.; Markus, E.; Antje, W. Thermal energy storage, overview and specific insight into nitrate salts for sensible and latent heat storage. *Belstein Journal of Nanotechnology.* ***2015.***

[2] Patricia, A.; Rosa, M.; Leonor, H.; Raul, M.; Luis, C.; J Enrique, J. Increment of specific heat capacity of solar salt with SiO2 nanoparticles. *National library of Medicine*. **2014.**

[3] Shin, D., Banerjee, D. Experimental Investigation of Molten Salt Nanofluid for Solar Thermal Energy Application. 8th Thermal, Engineering Joint Conference AJTEC. *ResearchGate*. **2011.**

This abnormal enhancement in the specific heat of the solar salts opens a new avenue of research and the unknown factors of this effect are currently being studied. The type of interaction between nanoparticles and solar salts is still unknown and several mechanisms for abnormal enhancement have been proposed. In this work we are going to study this kind of interactions using Quantum mechanics tools.

Within chemistry, Quantum mechanics (QM) is an essential tool for studying chemical reactions. Classical mechanics fails in describe correctly systems as small as electrons, which are very light particles. For this reason, quantum mechanics-based methods provide the best option to describe systems at the atomic scale. These methods involve a series of complex mathematical calculations which are carried out by computational resources. In this work we use these computational methods to study the reaction of silica nanoparticles 10 %wt (SiO_2) and his interaction with solar salts mixtures ($NaNO_3$:KNO_3) in order to enhance the heat capacity of the latter.

3. METHODOLOGY

In this section we will review all the mechanisms we have used to carry out this work.

3.1 Self-Consistent Field Method

In quantum mechanics we can describe the complete behaviour, in a no-relativistic way, of a molecular system using the time dependent Schrödinger equation, which can be written as:

$$\hat{H}\Psi = i\,\hbar\frac{\partial\Psi}{\partial t} \qquad [1]$$

where $\hat{H}$ is the Hamiltonian and Ψ the wave function of the system. This wave function is very important since it provides complete information about the system, being possible to calculate the density probability distribution of the particles with its square. The behaviour of Ψ is determined by the Hamiltonian operator, which also includes other operators to describe the system.

Considering the atom and the electrons as point masses we can separate in different terms the energy of both. The time-independent Hamiltonian can be written as [4]:

$$\hat{H} = \hat{T} + \hat{V} = \hat{T}_n + \hat{T}_e + \hat{V}_{nn} + \hat{V}_{ee} + \hat{V}_{ne} \qquad [2]$$

where *e* refers to electrons and *n* to the nuclei. The last term of equation is the potential energy of attraction between electrons and nuclei. Third and fourth terms refer to potential energy between electrons and between nuclei, in this case of repulsive nature.

[4] Peter, A.; Ronald F. Molecular Quantum Mechanics, 4th Edition. *Oxford University Press.* **2005.** *pp.288-319.*

Finally, the first and second terms correspond to kinetic energy of both, electrons and nuclei, separately.

Equation [2] can be solved for the Hydrogen atom, where the third and fourth are missing since there are just one proton and one electron, and the kinetic can be described by the relative movement of the electron to the proton. The solution of this equation gives a set of wavefunctions, known as hydrogen orbitals, which helps by extrapolation to understand the properties of the atom.

When it comes to find an analytical solution of equation [2] for polyelectronic atoms we deal with a more complex problem. For example, for the Helium atom with two electrons it's impossible to solve, and some assumptions must be made.

The first one is the Born-Oppenheimer approximation, that considers there is a big difference between electrons and nuclei, the mass ($M_n >> m_e$). Therefore, we can assume electrons are moving faster than the nuclei, fast enough to consider the latter static, and thus simplify the Hamiltonian neglecting the kinetic energy term of nuclei. This approximation also eliminates the correlation in attraction between electrons and nuclei, turning the nuclear repulsion into a classical Coulombic term, and simplifying the expression of the nuclei-electron attraction. The Hamiltonian can be rewrite now as:

$$\hat{H} = \hat{T}_e + \hat{V}_{ee} + \hat{V}_{ne} + V_{nn} \qquad [3]$$

where nuclear-nuclear repulsion term V_{nn} is reduced to a constant parameter given by the geometry.

The function now is separated in two parts, as the wavefunction describes exclusively the electrons of the system and thus, it depends of the nuclei coordinates. This leads to the following equation:

$$\hat{H}_{el}(R;r)\,\Psi_{el}(R;r) = E_{el}\Psi_{el}(R;r) \qquad [4]$$

$$E_{tot} = E_{el} + V_{nn}(R) \qquad [5]$$

where R and r refers to the coordinates of nuclei and electrons, respectively.

Therefore, the Hamiltonian obtained for Helium is purely electronic and can be written as:

$$\hat{H}_{el} = \hat{T}_1 + \hat{T}_2 + \hat{V}_{n,1} + \hat{V}_{n,2} + \hat{V}_{1,2} \qquad [6]$$

where the terms for each electron are expressed (1 and 2). The problem arises with the last term, which corresponds to the electron repulsion. This term makes it impossible to solve the equation by a variable separation method and to obtain an analytical solution for the problem.

A work around is to express the electronic system wavefunction as a combination of wavefunctions for each of the electrons in the system and try to approximate the repulsions between them.

This assumption requires to satisfy the Pauli exclusion principle (principle of antisymmetry) since the electrons are fermions and thus, are indistinguishable and identical particles. In order to satisfy the Pauli principle, the Slater determinants [5] are used. These determinants allow us to apply the HF method to systems with N electrons satisfying the antisymmetry principle.

This model takes the electron as a charge distributed in space (charge cloud model). This space is defined by the orbital of the electron and the probabilities of find that electrons are also distributed in this space. This one electron functions (Ψ_i) are known as spin-orbitals and are composed by a spatial and spin terms [6]. A slater determinant for N electrons can be written as:

$$\Psi = \frac{1}{\sqrt{N!}} \begin{vmatrix} (\Psi_1)(r_1) & (\Psi_2)(r_1) & \dots & (\Psi_N)(r_1) \\ (\Psi_1)(r_2) & (\Psi_2)(r_2) & \dots & (\Psi_N)(r_2) \\ \dots & \dots & \dots & \dots \\ (\Psi_1)(r_N) & (\Psi_2)(r_N) & \dots & (\Psi_N)(r_N) \end{vmatrix} \quad [7]$$

where each one of the N electrons can be described by each one of the spin-orbitals (Ψ_i) which conform the wave function of the polyelectronic system, providing a particular electronic configuration.

Regarding to the treatment of electronic repulsions, the most appropriate methodology is the so-called Self Consistent Field Method, initially proposed by Hartree and subsequently modified by Fock. In this method the system is reduced to a set of mono-electronic problems, the electrons of the system are threated sequentially, considering that each electron moves in an average electrostatic field generated by the rest of the electrons, which are static. As a result, an improved wave function is obtained for that electron, which will be reused in the subsequent resolution of the rest of the electrons of the system. The overall process ends when the changes in the wave function of the system (Ψ) are below a certain tolerance. Usually its square ($|\Psi^2|$), which provides the electron density, is taken as a reference.

Returning to the Helium atom [7], which fundamental electronic configuration is $1s^2$, the Slater determinant would be:

[5] The Sherrill Group, Computational Chemistry, An Introduction to Hartree-Fock Molecular Orbital Theory: Slater Determinants via http://vergil.chemistry.gatech.edu/notes/hf-intro/node4.html **(11/07/2020).**

[6] Emilio, S. F. M.; Juan Ferrer, C. Cálculos Computacionales (Teóricos) de Estructuras Moleculares, Tesis de la Universidad de Alicante, **2020.** *pp.8-13.*

[7] Quantum Mechanics in Chemistry, Second Edition, Melvin W. Hanna. **1969.** pp.115-140.

$$\Psi = \frac{1}{\sqrt{2}}\begin{vmatrix}\psi_1(r_1)\alpha_1 & \psi_2(r_1)\beta_1 \\ \psi_1(r_2)\alpha_2 & \psi_2(r_2)\beta_2\end{vmatrix} = \frac{1}{\sqrt{2}}\{\psi_1(r_1)\alpha_1 \cdot \psi_2(r_2)\beta_2 - \psi_2(r_1)\beta_1 \cdot \psi_1(r_2)\alpha_2\}$$ [8]

considering that $\psi_1 = \psi_2 = 1s = \psi$, we can rewrite:

$$\Psi = \frac{1}{\sqrt{2}}\psi(r_1) \cdot \psi(r_2) \cdot \{\alpha_1 \cdot \beta_2 - \beta_1 \cdot \alpha_2\}$$ [9]

Since the Hamiltonian does not contain spin terms, the equation is reduced to the product of the space parts (also known as Hartree product). The Hamiltonian for Helium atom can be written as follows (in atomic units):

$$\left(\hat{h}_1 + \hat{h}_2 + \frac{1}{r_{1,2}}\right)(\psi_1 \cdot \psi_2) = E \cdot (\psi_1 \cdot \psi_2) \qquad \hat{h}_i = -\frac{1}{2}\nabla_i^2 - \frac{Z}{r_i}$$ [10]

using the average repulsion between electrons, we can separate equation [9] in two different equations for each electron (i) and the iteraction achieved (k):

$$-\frac{1}{2}\nabla_i^2\psi_i^k - \frac{Z}{r_i}\psi_i^k + \psi_j^k\frac{1}{r_{i,j}}\psi_j^k\psi_i^k = \varepsilon_i^k\psi_i^k$$ [11]

Initially, the problem for the first electron is solved, obtaining the energy (ε_1^1) and a more approximated wavefunction (ψ_1^1), compared to the initial system (ψ_1^0, ψ_2^0):

$$-\frac{1}{2}\int \psi_1^1\,\nabla_1^2\psi_1^1 - \int \psi_1^1\frac{Z}{r_1}\psi_1^1 + \int \psi_1^1\,\psi_2^0\frac{1}{r_{1,2}}\psi_2^0\psi_1^1 = \varepsilon_1^1$$ [12]

Then, this new wavefunction is used to refine the second-one:

$$-\frac{1}{2}\int \psi_2^1\,\nabla_2^2\psi_2^1 - \int \psi_2^1\frac{Z}{r_2}\psi_2^1 + \int \psi_1^1\,\psi_2^1\frac{1}{r_{1,2}}\psi_2^1\psi_1^1 = \varepsilon_2^1$$ [13]

This process is repeated until the changes in electron density are below a certain threshold (k=m). The final energy cannot be obtained directly from the sum of the energies of each electron, since the electron pair repulsion would be considered twice:

$$E = \varepsilon_1^m + \varepsilon_2^m - \int \psi_1^m\,\psi_2^m\frac{1}{r_{1,2}}\psi_2^m\psi_1^m$$ [14]

We have exposed the simplest case of a polyelectronic atom. In the case of having molecules, formed by two or more atoms, the procedure is similar. The molecular wave function is expressed as a Slater determinant containing as much spin-orbitals as electrons.

3.2 Base functions

Instead of using hydrogen wave functions in the Slater determinants, other kind of base functions are used for reasons of computational efficiency. In this work we use adjustments of Gaussian functions of the radial parts of the hydrogen orbitals.

These orbitals can be written as a product of a linear combination of Gaussian functions (GTO), which allow a faster calculation for the molecular integrals:

$$GTO = \frac{2\chi}{\pi^{\frac{3}{4}}} \cdot e^{(-\chi * r^2)} \qquad [15]$$

The basis sets equations based by the Slater Type Orbitals (STO) are considered minimal basis sets [8]. The most common in this group is the STO-nG. Where n is an integer that indicates the number of Gaussian functions included in the same basis function. This primitive Gaussian functions also include valence and core orbitals. This kind of basis sets typically don't give very good results compared to their larger counterparts. The most commonly minimal basis sets used are the STO-6G.

Split-valence basis sets: in a bonding between two atoms are the valence electrons which mainly involved. In view of that, it is common represent with more than one basis functions the valence orbitals. The most commonly known split-valence sets are 6-31G.

The nomenclature of this basis sets is important to understand how it works. The first number refers to the number of Gaussian functions summed to describe inner shell. The second number represents the number of Gaussian functions that compromise the first STO of the Double zeta. The last number shows the number of Gaussian summed to the second STO. For **6-31G** we have respectively:

- **6** Gaussian functions describing the inner-shell-orbital.
- **3** Gaussian functions for the first Slater type orbital.
- **1** Gaussian function for the second Slater type orbital.

In addition to split-valence and minimal basis sets we can add **polarization functions**, which describe polarization of the electron density of the atom in molecules. This basis sets incorporate functions to atoms with higher angular momenta that are required for the description of the ground state. In order to represent these functions, the asterisks have been used, where one asterisk means that polarization has been considered in the *d* orbital (heavy atoms), meanwhile two asterisks refers an additional polarization in *p* orbitals for hydrogen atoms.

[8] Wikipedia: Basis sets (Chemistry). Split-valence basis sets, Polarization-consistent basis sets and Pople basis sets *via* https://en.wikipedia.org/wiki/Basis_set_(chemistry) **(11/07/2020).**

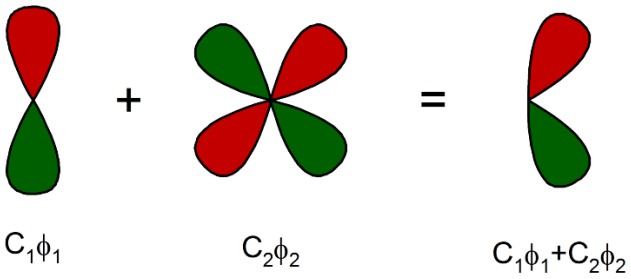

Figure 1. A d-polarization function added to a p orbital. [8]

There are other type of basis sets that are commonly added to the calculations, the **diffuse functions**. That kind of functions are important to describe anions or dipole moments and provide a more accurate result. This kind of orbitals occupy a larger region in space and improve the description of species with extended electronic densities, as we said, anions or molecules forming hydrogen bonds. The presence of this orbitals is represented by one or two '+' in the basis set name. An example could be 6-31++G* which indicates the presence of diffuse functions on hydrogen atoms.

3.3 Density Functional Theory

One of the main problems of molecular orbital methods like Hartree Fock is the lack of correlation in the electron movement. The reason is because each electron is solved in an individual way, leaving the rest of the electrons of the system in a fixed position. Doing this type of approximation, we lose the component corresponding to the relative motion of the electrons and the dynamic interactions between them. There are several methods, called post Hartee-Fock, that allow to correct this mistake by means of different approximations. Among them, there are those based on the functional of electronic density.

Density functional theory (DFT) is an alternative method which uses the electron density, $\rho(r)$, as the principle variable. The electron density has the advantage over the wave function that, only depends on spatial coordinates (*x,y,z*) and the spin, whereas the wave function not only depends on spin but also on 3N variables, being N the number of electrons in the system. The key to the DFT arises from the way the electrons that give rise to a certain density value are considered, being reduced to a dynamically equivalent system of non-interacting N electrons.

The expression of the energy for a system in terms of electron density ρ(r), under the Born-Oppenheimer approximation, can be written as [9]:

$$E[\rho(r)] = T_{ni}[\rho(r)] + V_{n,e}[\rho(r)] + V_{e,e}[\rho(r)] + V_{n,n}(R) + \Delta T[\rho(r)] + \Delta V_{e,e}[\rho(r)] \quad [16]$$

[9] Kaupp, M. Book Review: A Chemist's Guide to Density Functional Theory. By Wolfram Koch and Max C. Holthausen. *Angewandte Chemie International Edition*, 40(5). **2001**. pp.963-964.

where the first term, $T_{ni}[\rho(r)]$, refers to the kinetic energy of the non-interacting electrons; the second one, $V_{n,e}[\rho(r)]$, corresponds to the interaction between nuclei and electron. The third term, $V_{e,e}[\rho(r)]$, accounts for the repulsion between electrons, and the fourth one, $V_{n,n}(R)$ reflects the classical repulsion between nuclei. The fifth term, $\Delta T[\rho(r)]$, is the correction to the kinetic energy deriving from the interacting nature of the electrons, and finally, last term, $\Delta V_{ee}[\rho(\vec{r})]$, accounts for all non-classical contributions to the repulsion between the electrons [10].

The last two terms are grouped together leading to the exchange-correlation potential, $V_{XC}[\rho(r)]$, which contain all the unknown terms and, which is approximated by a certain analytical functional of the electron density:

$$E[\rho(r)] = T_{ni}[\rho(r)] + V_{n,e}[\rho(r)] + V_{e,e}[\rho(r)] + V_{n,n}(R) + V_{XC}[\rho(r)] \qquad [17]$$

Generally, the exchange-correlation potential is expressed by the sum of every contribution:

$$V_{XC}[\rho(r)] = V_X[\rho(r)] + V_C[\rho(r)] \qquad [18]$$

There are different expressions available for the terms involved in equation [18], such as:

- Local density approximation (LDA): this model focuses on the idea of a hypothetical uniform electron gas, known as homogeneous electron gas, which is distributed in a positive charged background, obtaining a total electrically neutral assembly. This system is possible because the DFT allows to know the form of the exchange and correlation energy functionals with a very high degree of accuracy.
- Generalized gradient approximation (GGA): the GGA methods use not only the information about density $\rho(r)$, but they also include information about the gradient of the charge density ($\nabla\rho$).

The most used GGA correlation functionals are:

- **LYP**[11]: correlation functional of Lee, Yang and Parr, which includes local and non-local terms.
- **PBE**[12]: gradient-corrected correlation functional of Perdew, Burke and Ernzerhof.

[10] M. A.L. Marques. Book review: A Primer in Density Functional Theory by C. Fiolhais, F. Nogueira and M. Marques. *Springer.* **2010.**

[11] C. Lee.; W. Yang.; R. G. Parr. "Development of the Colle-Salvetti correlation-energy formula into a functional of the electron density", *Phys. Rev. B*. **1988**, 37, pp.785-789.

[12] J. P. Perdew.; M. Ernzerhof.; K. Burke. "Rationale for mixing exact exchange with density functional approximations", *J. Chem. Phys*., **1996** 105, 9982.

Regarding the exchange functional, the most commonly used is the Becke's functional **B**[13], which also includes Staler corrections for the gradient of the density.

The most recent functionals called meta-GGA belong to this family of functionals, but they incorporate higher-order density gradient terms.

Finally, Hybrid functionals combine the exchange-correlation of conventional GGA or M-GGA methods with a small percentage of pure HF exchange. The current amount of this last parameter is fitted empirically. There are many exchange-correlation hybrid-GGA functionals. One of the most widely used is **B3LYP**, the Becke three parameter Lee-Yang-Parr functional:

$$E_{XC}^{B3LYP} = (0.20E^{HF} + 0.72E^{B88,GGA} + 0.08E^{S,LDA})_X + (0.81E^{LYP,GGA} + 0.19E^{VWN-3/5,LDA})_C \quad [19]$$

where, as we can see, LDA functionals are also used: Slater (S [14]) for the exchange, and Vocko, Wilk and Nusair (VWN [15]) for the correlation.

In conclusion, DFT is a powerful tool which can provide similar or even better results than methods based on wave function, also with lower computational cost. It has a disadvantage: if a selected functional provides a wrong result, it can't be systematically improved. Even so, DFT is one of the most used methods in calculating the structures of molecules and chemical reactivity in computational chemistry.

3.4 Functionals: B3LYP

B3LYP is one of the most popular density functional in computational chemistry. This hybrid functional was one of the first DFT methods which gave a significant improvement over HF methods. B3LYP is generally faster than most post Hartree-Fock techniques and usually brings similar results. It is also fairly robust for a DFT method, with a not very high computation cost. On a more fundamental level, it is not as heavily parameterized as other hybrid functionals, having only 3. Although another hybrid functionals have been commonly used in recent times, as the Minnesota suite of density functionals, B3LYP is still one of the most used and one of the most balanced hybrid functionals in terms of cost of the calculations and quality of the results.

[13] A. D. Becke. "Density-functional exchange-energy approximation with correct asymptotic behaviour", *Phys. Rev. A* **1988**, 38, pp.3098-3100.
[14] J. C. Slater, The Self-Consistent Field for Molecular and Solids, Quantum Theory of Molecular and Solids, Vol. 4 (McGraw-Hill, New York, **1974**).
[15] S. H. Vosko, L. Wilk, and M. Nusair, "Accurate spin-dependent electron liquid correlation energies for local spin density calculations: A critical analysis," *Can. J. Phys*., 58 (**1980**) pp.1200-1211

In the year 2019 a total of 10724 articles were published where DFT methods were applied, in more than one third of these articles (34.9%) B3LYP is used as a hybrid functional [16].

The following graph shows the total number of articles in 2019 where DFT methods were used and where B3LYP was used as a functional hybrid. The use in the total number of articles and in different study topics is shown:

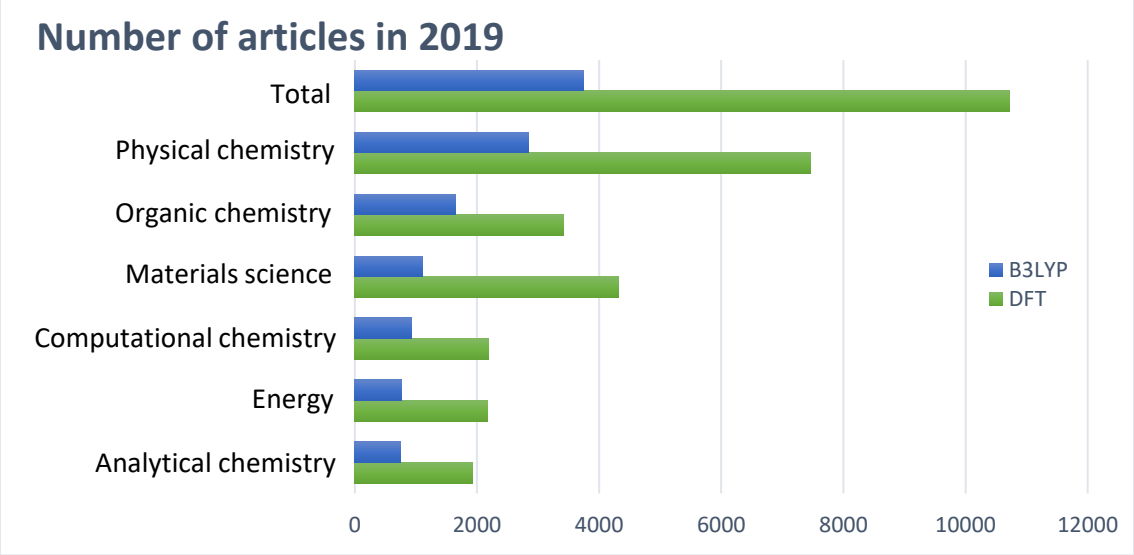

Graphic 1. Amount of B3LYP usage in DFT methods in 2019.

3.5 Gibbs free energy: RRHO

The value of the free energy associated to a certain chemical process gives us information about it, such as its degree of spontaneity (either endergonic or exergonic), or the proportion that will be established between the reagents and products when the equilibrium is reached (equilibrium constant). Since mechano-quantum calculations provide the internal energy of the system, additional methods are needed to estimate the free energy of the system, usually based on statistical thermodynamics. Initially, we can use Maxwell's relationship between Gibbs' energy and Helmholtz's potential:

$$G = F + PV \qquad [20]$$

Then, we must apply some considerations:

- The energy of the different levels will be expressed according to the energy of the fundamental level, which will become zero. Doing that, the partition function of the system when only the fundamental level is populated will be equal to the unity (it would correspond to the case when the temperature is 0 K).

[16] B3LYP and DFT methods search (filter: last year) via *https://pubs.acs.org/* **(12/07/2020).**

- We introduce the relationship between Helmholtz potential and the canonical partition function of system Q_{NVT}, derived from the statistical definition of entropy:

$$F - F(0) = -k_B T \ln Q \qquad [21]$$

- We will assume that the system has an ideal behaviour (particles are independent and indistinguishable):

$$Q = \frac{q^N}{N!} \qquad [22]$$

- The energy value when the temperature is 0 K is independent of the variables that control the measurement (or collective):

$$G(0) \approx F(0) \approx U(0) \qquad [23]$$

- The Stirling approximation [17] to approximate the logarithm value of a factorial for a large number:

$$\ln N! \approx N \ln N - N \qquad [24]$$

With these assumptions we can write the Gibbs free energy as:

$$G^o \approx U^o(0) - RT \ln\left(\frac{q}{N_A}\right) \qquad [25]$$

where the partition molecular function q (equation [22]) can be obtained from the expressions derived for the ideal gas case:

$$\varepsilon = \varepsilon_{tras} + \varepsilon_{rot} + \varepsilon_{vib} + \varepsilon_{ele} \qquad q = q_{tras} \cdot q_{rot} \cdot q_{vib} \cdot q_{ele}$$

$$q_{tras} = \left(\frac{2\pi m k_B T}{h^2}\right)^{\frac{3}{2}} V \qquad q_{rot} = \frac{\sqrt{\pi}}{\sigma} \frac{T^{\frac{3}{2}}}{\sqrt{\theta_A \theta_B \theta_C}} \qquad \theta_i = \frac{h^2}{8\pi^2 k_B I_i} \qquad [26]$$

$$q_{vib} = \prod_i^{nmodes} \frac{1}{1 - e^{-\frac{h\upsilon_i}{k_B T}}} \qquad q_{ele} = \sum_i^{states} g_s e^{\frac{-\varepsilon_i}{k_B T}}$$

This approximation is commonly known as Rigid Rotor Harmonic Oscillator (RRHO).

[17] Wikipedia, Stirling approximation via https://en.wikipedia.org/wiki/Stirling%27s_approximation **(12/07/2020).**

3.6 IR spectrum

Quantum mechanics provides a simple solution to the problem of vibration for a diatomic molecule, which is described as a single particle with reduced mass m = $\frac{m1 \cdot m2}{(m1 + m2)}$ (kg) attached to a spring:

$$E = h\upsilon\left(v + \frac{1}{2}\right) \qquad \upsilon = \frac{1}{2\pi}\sqrt{\frac{k}{m}} \qquad [27]$$

where $\mathcal{V}$ is the corresponding vibrational quantum number ($\mathcal{V}$ = 0, 1, 2, ...), υ is the frequency of the oscillator (s^{-1}) and *k* is the force constant related to the strength of the chemical bond (N/m). A difference from the classical result is that the energy is not zero when $\mathcal{V}$ =0, we obtain a residual value equal to ½hu, known as zero-point energy (ZPE).

To study transitions between different vibrational states caused by the absorption of electromagnetic radiation, we must look at the dipole moment operator of the molecule, as it is the most appropriate one to describe the interaction of the molecule with the radiation (with the electric field component). In addition, we must take into account that this dipole moment will vary with the molecular vibrations associated with each vibrational state. If we consider that these variations are small, we can express the dipole moment operator as a Taylor series of a few terms:

$$\hat{\mu} = \mu_e + \left(\frac{\partial \mu}{\partial R}\right)_{R_e}(R - R_e) + \frac{1}{2}\left(\frac{\partial^2 \mu}{\partial R^2}\right)_{R_e}(R - R_e)^2 + \cdots \qquad [28]$$

where R_e represents the equilibrium distance of the diatomic molecule and μ_e is the electronic component of dipolar moment. Thus, the dipole moment of the transition between two vibrational states v'' and v' is:

$$\int \Psi^*_{v'}\hat{\mu}\Psi_{v''}d\tau_{vib} \approx \mu_e \int \Psi^*_{v'}\Psi_{v''}d\tau_{vib} + \left(\frac{\partial \mu}{\partial R}\right)_{R_e}\int \Psi^*_{v'}(R - R_e)\Psi_{v''}d\tau_{vib}$$
$$|\mu|_{v'',v'} \approx \left(\frac{\partial \mu}{\partial R}\right)_{R_e}\int \Psi^*_{v'}(R - R_e)\Psi_{v''}d\tau_{vib} \qquad [29]$$

where the first integral is neglected due to the orthogonality condition of the vibrational wave functions and equation [28] has been simplified to the first term. So, equation [29] provides the conditions for the vibrational transition between the states v'' and v' mediated by absorption of electromagnetic radiation.

The dipole moment of the molecule must vary with the geometry during the transition, and will modulate its intensity:

$$\left(\frac{\partial \mu}{\partial R}\right)_{R_e} \neq 0 \qquad [30]$$

For the equation [29] a selection rule must be enforced in order to obtain a value different to zero:

$$\Delta v = v' - v'' = \pm 1 \qquad [31]$$

In the case of polyatomic molecules, the vibrations of the nuclei are more complex, but can be expressed as a linear combination of a finite number of independent vibrations, known as normal modes. In each of these normal modes the atoms vibrate in phase and with the same frequency (although the amplitude of this vibration may be different). Since the normal modes are orthogonal, vibrational energy and wave function can be expressed from them:

$$E_{vib} = h \sum_{i=1}^{nmodes} \upsilon_i \left(v_i + \frac{1}{2}\right)$$

$$\Psi_{vib} = \prod_{i=1}^{nmodes} \psi_{vib,i}(q_i) \qquad [32]$$

$$ZPE = \frac{h}{2} \sum_{i=1}^{nmodes} \upsilon_i$$

From a practical point of view, the value of k/m in equation [27] is obtained from the eigenvalues of the mass weighted matrix of the second energy-derived coordinates (Hessian matrix). In addition, it is common to use Lorentzian type [18] functions to simulate band widening when graphing the spectra:

$$L(\upsilon) = \sum_{k=1}^{nmodes} I_k \left(1 + \frac{\upsilon - \upsilon_{o,k}}{\omega_k/2}\right)^{-1} \qquad [33]$$

where I_k, $\upsilon_{o,k}$ and ω_k represent the intensity (equation [30]), frequency and bandwidth measured at half height (FWHM) of each of the normal modes of the molecule.

3.7 Heat capacity

Heat capacity can be derived from the expression of the internal energy of the system in terms of the partition function (equation [22]):

$$U = k_B T^2 \frac{\partial ln Q}{\partial T} \qquad U = k_B T^2 \frac{1}{Q}\frac{\partial Q}{\partial T} \qquad c_v = \left(\frac{\partial U}{\partial T}\right)_V$$

$$c_V = \left(\frac{\partial U}{\partial T}\right)_V \approx 3N_A k_B + N_A k_B \sum \frac{\theta^2}{T^2} \frac{e^{\frac{\theta}{T}}}{\left(e^{\frac{\theta}{T}} - 1\right)^2} \qquad \theta = h\frac{\upsilon_e}{k_B} \qquad [34]$$

where the first term in the c_v ($3 \cdot R$, $R = N_A \cdot k_B$) arises from the dependency of translational and rotational motions on $T^{3/2}$. Thus, the remaining term accounts for the different vibrational modes of the molecule, being θ the vibrational temperature of each mode. This last term is the responsible for the different value of the heat capacity among the given molecules (with translational, rotational and vibrational degrees of freedom).

[18] Wikipedia, Spectral line shape, Line shape functions: Lorentzian via *https://en.wikipedia.org/wiki/Spectral_line_shape* **(12/07/2020).**

4. RESULTS

In this work, a quantum chemical analysis has been carried to study the behaviour of silica nanoparticles when interacting with solar salts, in order to explain the reason for the increase in the heating capacity of the mixture. For this purpose, Gaussian09 calculations have been used, first to evaluate the mechanism of the silica clustering, and second to study the availability of the chemical interaction between these clusters and the solar salt. A DFT method has been used for this purpose with an extended basis set 6-31G(*d,p*) and the B3LYP as an exchange-correlation functional. We will also compare the experimental FTIR spectra with the theorical one for the solar salt, the nanoparticles and the nanofluid trying to assign each peak and determine whether if the introduction of a nitrate group is possible.

4.1 Mechanism of silica clustering

In order to understand the interaction between silica nanoparticles and solar salt we must first know the behaviour of silica in solution. The simplest soluble molecule of silica is the orthosilicic acid, $Si(OH)_4$. The orthosilicic acid undergoes self-polycondensation [19] in solution, where every interaction between two molecules will generate one molecule of water as is shown in ***Figure 2***:

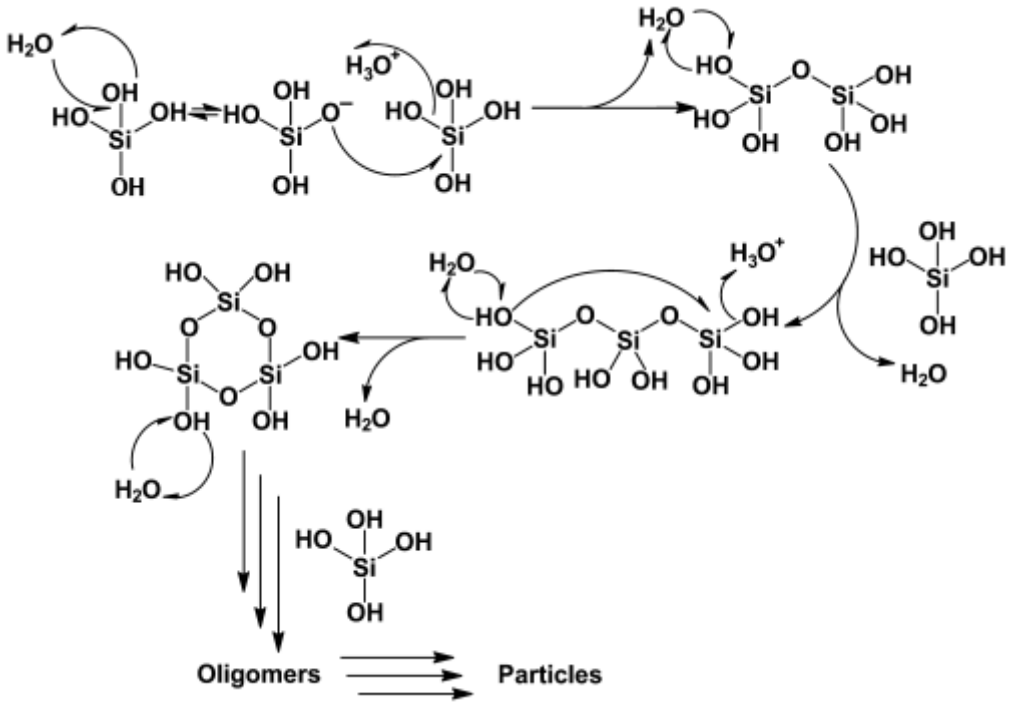

Figure 2. *Mechanism of condensation of silicic acid species in solution.*

[19] David J. B.; Olivier D.; Carole C. P. An overview of the fundamentals of the chemistry of silica with relevance to biosilicification and technological advances. *FebsPress.* **2012**.

From the 6 silicon atoms, small clusters of silica are formed. The simplest models are those of 6 and 8 silicon atoms, for which 9 and 12 water molecules are released respectively, one for each new Si-O bond formed. ***Figure 3*** shows some of the structures formed in the self-polycondensation of orthosilicic acid. From two silicon atoms to a cluster of eight silicons:

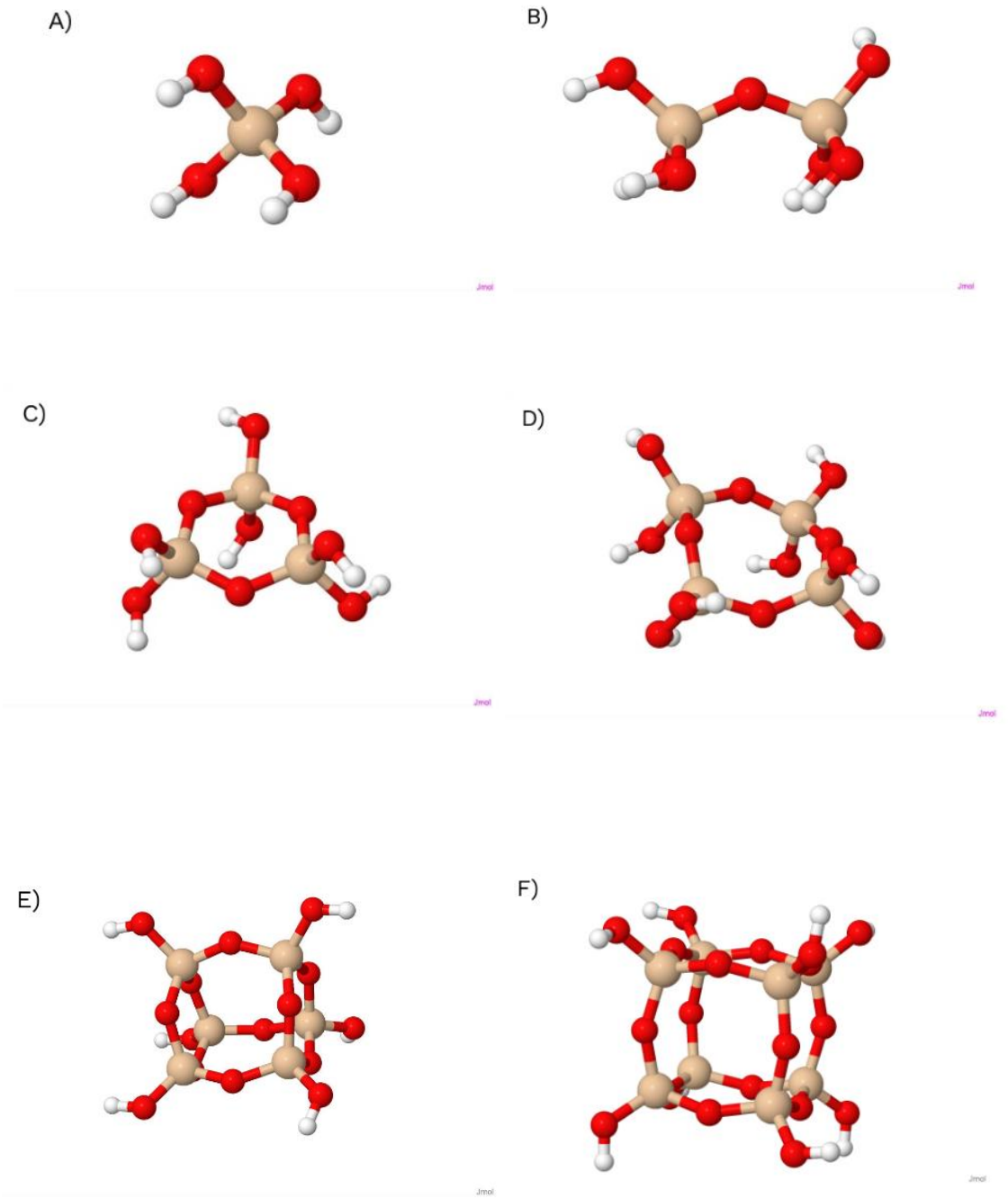

Figure 3. *Exemplary orthosilicic acid structures from monomers through to octamers. A) Orthosilicic acid, B) two silicon product, C) three silicon product, D) four silicon product, E) six silicon cluster and F) eight silicon cluster.*

In this work we will use the 6 and 8 silicon clusters as they are the two most representative models for silica nanoparticles.

In order to verify the behaviour of the nanoparticles in solution, some calculations have been made to check that small silica clusters of 6 and 8 silicon atoms are being formed. For this purpose, we have selected the combination of B3LYP/6-31G(d,p) for the calculations. First, an optimization of the molecules must be made:

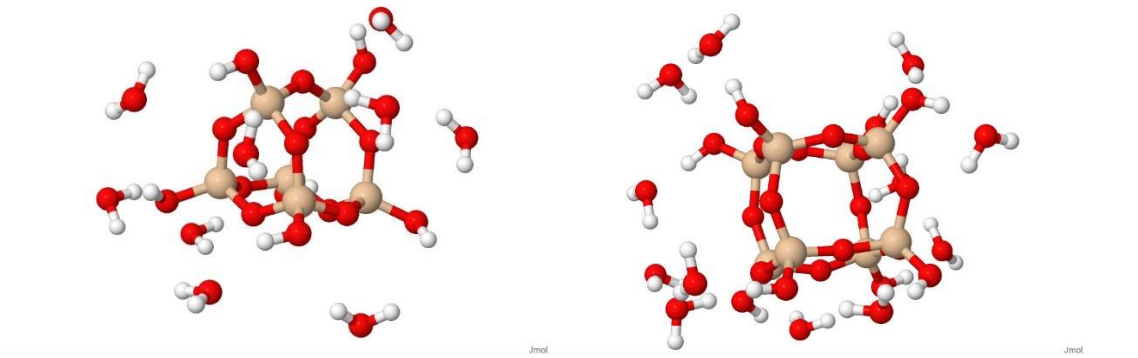

Figure 4. *Cluster model products of auto-polycondensation of orthosilicic acid.*

Once we have the correct geometry of the molecule its internal energy is calculated to obtain the Gibbs free energy, which will give us information about the formation of the silica clusters. In all the calculations very high equilibrium constants are obtained, which indicates the formation of the silica clusters.

- Reaction 6 silicon atoms:

$$\mathbf{6\ Si(OH)_4 \leftrightarrow Si_6O_9(OH)_6 + 9\ H_2O}$$

Nº Molecules	Molecule	E_o+Gcorr (Ha)
6	$Si(OH)_4$	-3558.632111
1	$Si_6O_9(OH)_6$	-3558.671893
9	H_2O	

Table 1. *Internal energies for the clustering of 6 silicon atoms (Ha).*

Once we have the energy of reagents and products, we must convert it from Hartrees to kJ/mol using the relationship:

$$1\ \text{Hartree} = 2625.5\ \text{kJ/mol} \qquad [33]$$

and calculate the Gibbs free energy (ΔG^o) as:

$$\Delta G^o = G_{products} - G_{reagents} \qquad [34]$$

With the ΔGº of the reaction, we can calculate the reaction constant as:

$$K_{eq} = e^{\frac{-\Delta G^{º}}{RT}} \quad [35]$$

where R is a constant and T is temperature (K). The results obtained are represented in the following table:

$\Delta G^{º}$ (kj/mol)	K_{eq}
-104.448	1.54×10^{18}

Table 2. *Equilibrium constant for* auto-polycondensation of 6 silicon atoms.

Applying same procedure to the 8 silicon atoms cluster:

- Reaction 8 silicon atoms:

$$\mathbf{8\ Si(OH)_4 \leftrightarrow Si_8O_{12}(OH)_8 + 12\ H_2O}$$

Nº Molecules	Molecule	E_o+G_{corr} (Ha)
8	$Si(OH)_4$	-4744,831496
1	$Si_8O_{12}(OH)_8$	-4744,930549
12	H_2O	

Table 3. *Internal energies for the clustering of 6 silicon atoms (Ha).*

$\Delta G^{º}$ (kj/mol)	K_{eq}
-260.064	1.92×10^{45}

Table 4. *Equilibrium constant for* auto-polycondensation of 8 silicon atoms.

The results shown in ***Table 2*** and ***Table 4*** demonstrate that this is a very exothermic reaction where orthosilicic acid spontaneously forms clusters of 6 and 8 silicon from self-condensation, where for each new Si-O bond formed, one water molecule is released.

4.2 IR spectrum

Once we have the silica cluster model and the solar salt model, we can obtain their theoretical vibration frequencies, and with them the corresponding theoretical spectrum. It is important to take into account the error made by the method and basis set used [20]. Comparing this theoretical spectrum with the experimental one we will be able to verify what is happening in the interaction between the solar salt and the silica.

Figure 5 and ***Figure 6*** show both, the theoretical and the experimental spectrum respectively for nanoparticles, salt and mixture. The experimental spectrum has been provided by Rosa Mondragon and her team who are also studying this field:

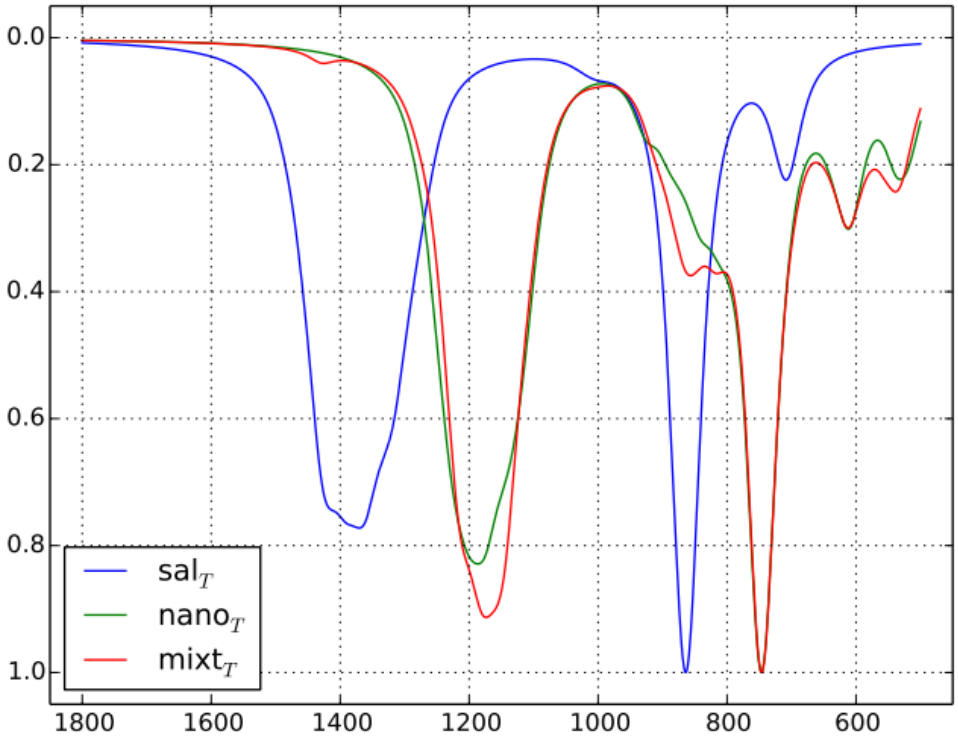

Figure 5. *IR theoretical spectrum for nanoparticles, salt and mixture.*

[20] IR frequencies have been scaled considering the errors of the theoretical method and basis set used, as described in *https://cccbdb.nist.gov/vibscalejust.asp* **(14/07/2020).**

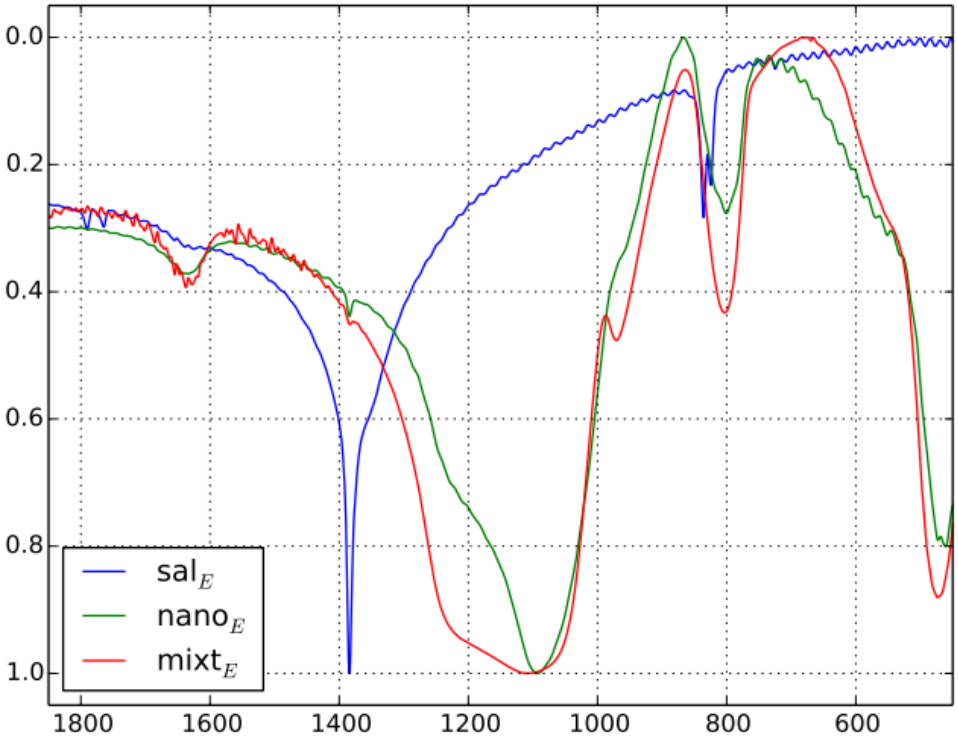

Figure 6. *IR experimental spectrum for nanoparticles, salt and mixture.*

4.2.1 IR silica cluster

First, we must obtain the spectrum for the reagents. For silica nanoparticles, we have used the eight-silicon cluster since it is the most representative model (the largest one). As we have explained before, orthosilicic acid undergoes self-polycondensation in solution forming silica clusters. For each Si-O link formed, one water molecule is released. So, in the case of the eight-silicon cluster, 12 water molecules will be released as shown in the following figure:

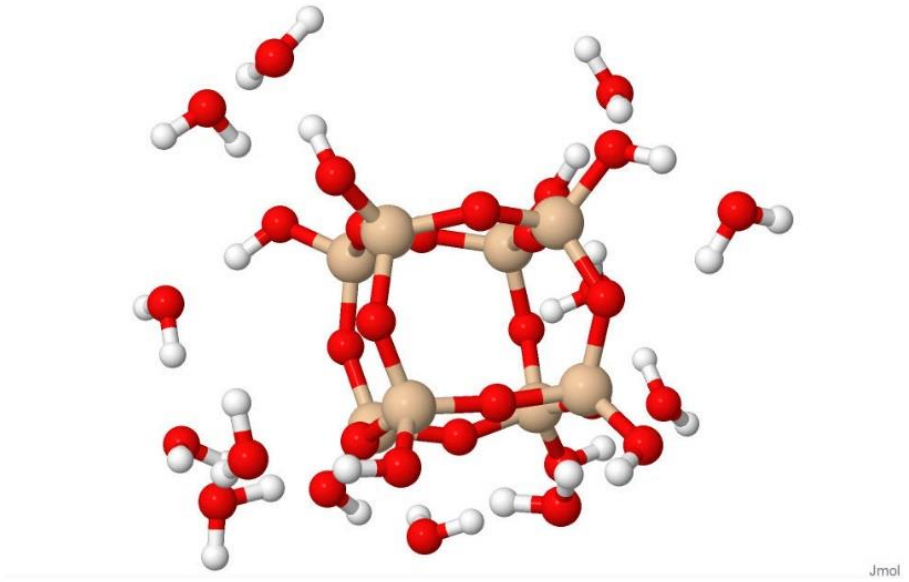

Figure 5. *Cluster silica product.*

Once we have the model of the eight-silicon cluster, we can obtain its vibration frequencies and from them represent the IR spectrum of the model. In the following figure we can observe the theorical spectrum of the eight-silica cluster (blue line) superposed with the experimental one (green line):

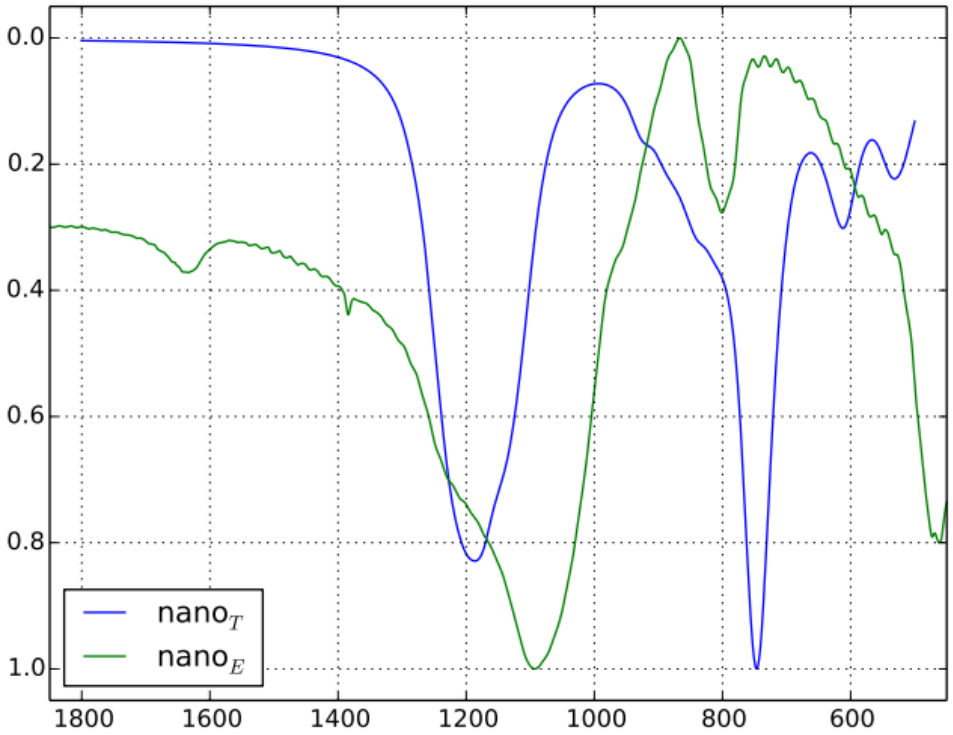

Figure 6. *IR silica cluster.*

In the following table are compiled all the vibration frequencies in cm^{-1} of the silica cluster surrounded by the twelve water molecules, as well as the assignment of each vibration:

Signal	Frequency (cm^{-1})	Assignment
A	1636	H_2O molecules
B	1632	H_2O molecules
C	1141	Si-O-Si stretching
D	993	Si-OH stretching
E	958	Si-OH stretching
F	804	Si-O-Si stretching
G	542	Si-O-Si stretching

Table 5. *Frequencies silica cluster.*

The peak over 1630 cm^{-1} (A and B signals) corresponds to the vibrations of the water molecules. The silica cluster theoretically has three characteristic bands, two bands on 1090-1010 cm^{-1} (C signal) and another on 625-480 cm^{-1} (F and G signals) that correspond

to the Si-O-Si stretch and third band on 955-830 cm^{-1} (D and E signals) that corresponds to the Si-OH stretching [21].

4.2.2 IR solar salt

The solar salt model is composed of a network of nitrate anions and metal cations as shown in the figure below:

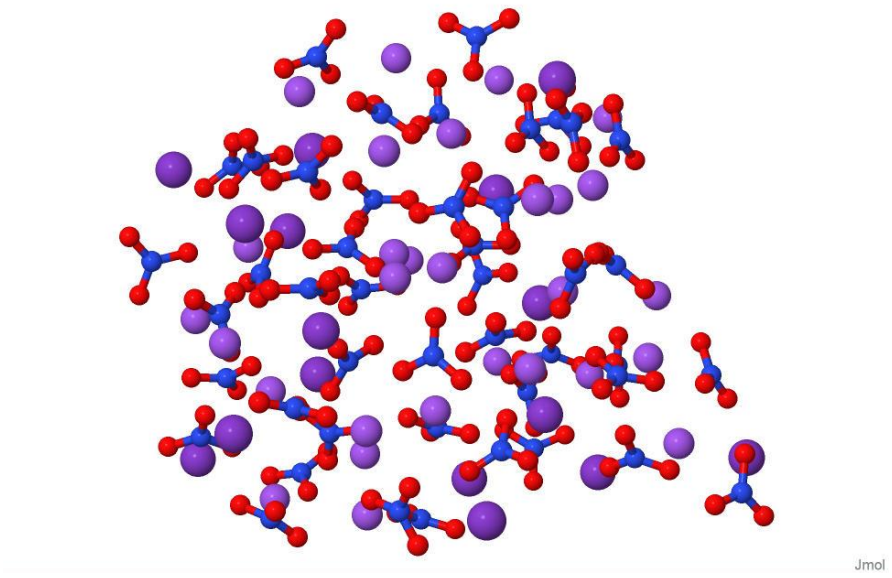

Figure 7. *Solar salt.*

For this model we have used a total of 16 molecules of KNO_3 and 29 molecules of $NaNO_3$ to obtain a mixture 40:60 %wt of K^+/Na^+.

The theoretical spectrum of the solar salt is obtained in the same way as with the eight-silicon cluster and is represented in the following figure (blue line) together with the experimental spectrum (green line):

[21] Infrared and Raman Characteristic Group Frequencies, Third Edition, JOHN WILEY & SONS. **2001.** pp.243-246.

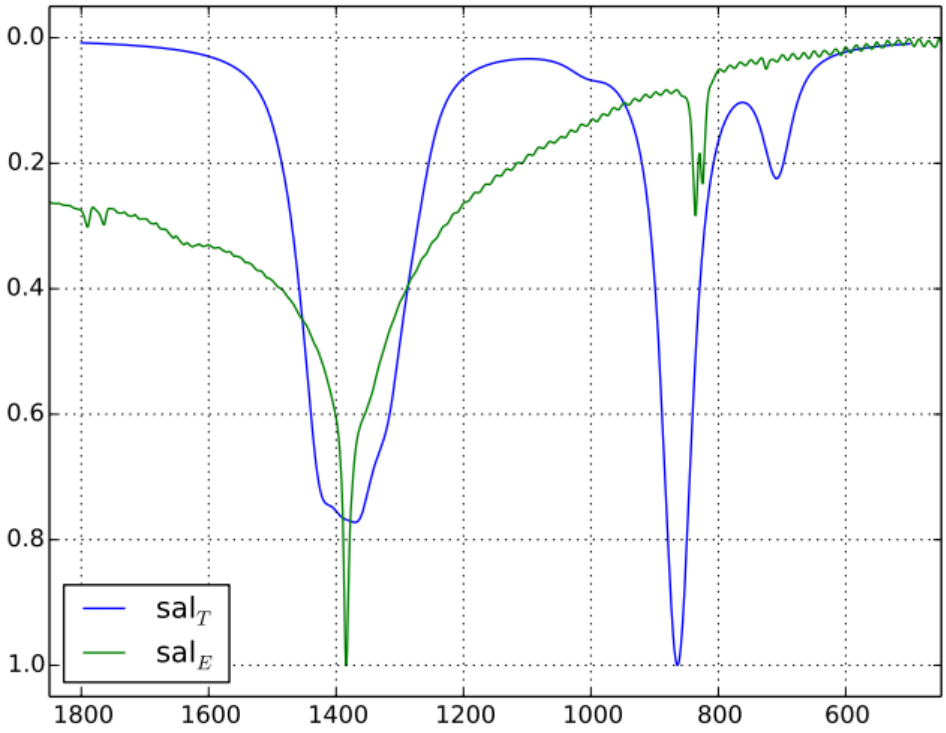

Figure 8. *IR solar salt.*

The following table shows all the vibration frequencies of the solar salt, as well as the assignment for each of these vibrations:

Signal	Frequency (cm^{-1})	Assignment
A	1396	N-O stretching
B	859	N out-of-plane bending
C	865	N out-of-plane bending

Table 6. *Frequencies solar salt.*

Inorganic nitrates commonly present two characteristic bands, one on 1450-1340 cm^{-1} and the other on 825 cm^{-1} both corresponding to the N-O stretching and N out-of-plane bending respectively.

In the following figure are represented the vectors of movement for each vibration for the solar salt model:

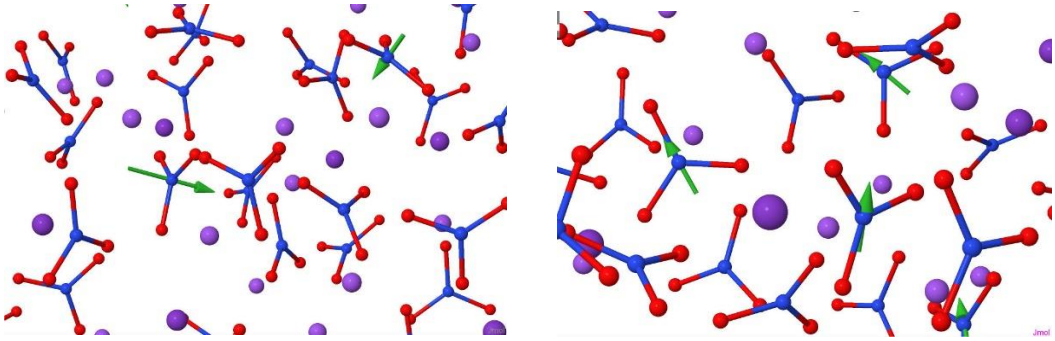

Figure 9. *Vectors of movement of N out-of-plane bending and N-O stretching respectively.*

4.2.3 IR nanofluid

Once we obtain the IR of the two reagents and verify that the theoretical spectra agree with the experimental ones, we must propose a model for the products. In our case we have proposed two models: one where the silica cluster is found inside the solar salt (without chemical reaction) and another where a nitrate group is included in the nanoparticle (with chemical reaction). Due to the size of the system, an initial concentration of nanoparticles of 10 %wt has been selected, although it experimentally determined that the optimal concentration providing a larger increase on the heat capacity is around 2 %wt, since it is known that it is the mass percentage that provides a greater increase of the specific heat because of the contact surface of the nanoparticle, which is maximum due to the lack of agglomerations.

For this model we have used a total of 16 molecules of KNO_3, 25 molecules of $NaNO_3$ and, for the nanoparticles, an eight-silicon cluster.

The following figure corresponds to the first model where the silica cluster remains unreacted to the solar salt:

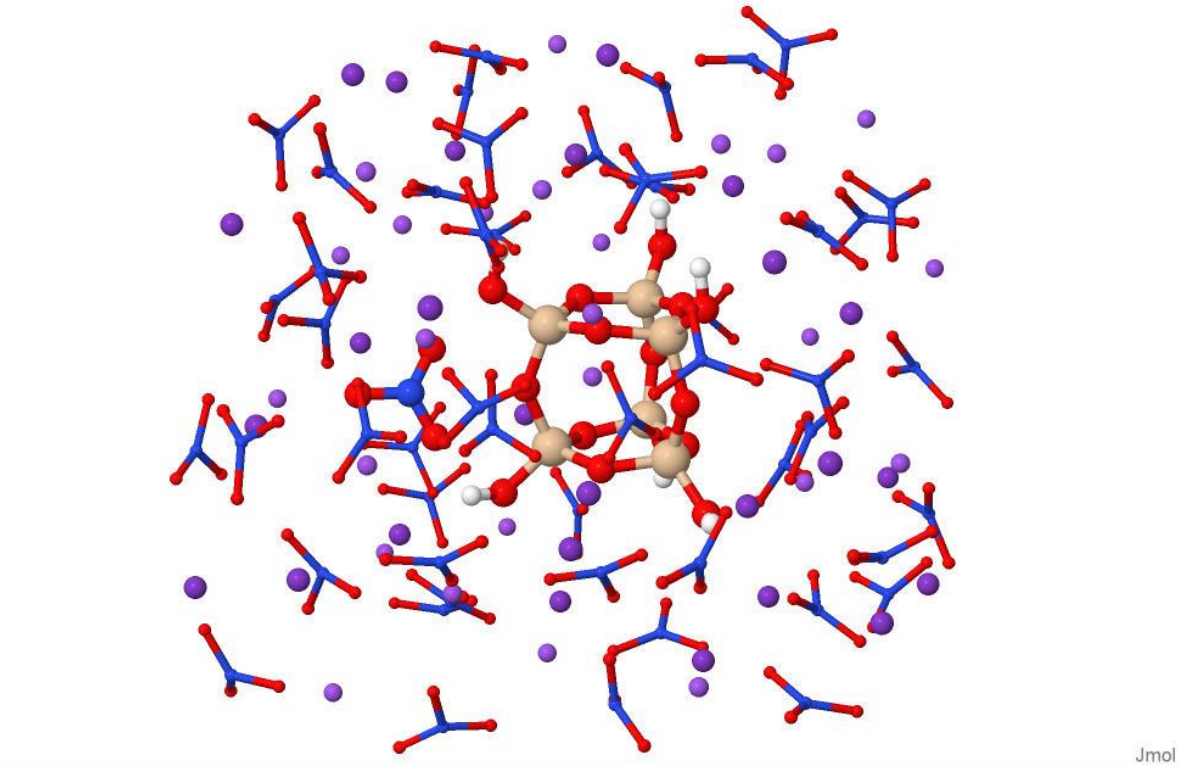

Figure 10. *Solar salt silica cluster interaction without chemical reaction.*

The theoretical IR spectrum (blue line) is represented together with the three experimental spectra as is shown in ***Figure 11***: experimental solar salt spectrum (blue dotted line), experimental silica cluster spectrum (purple dotted line) and experimental nanofluid spectrum (red dotted line).

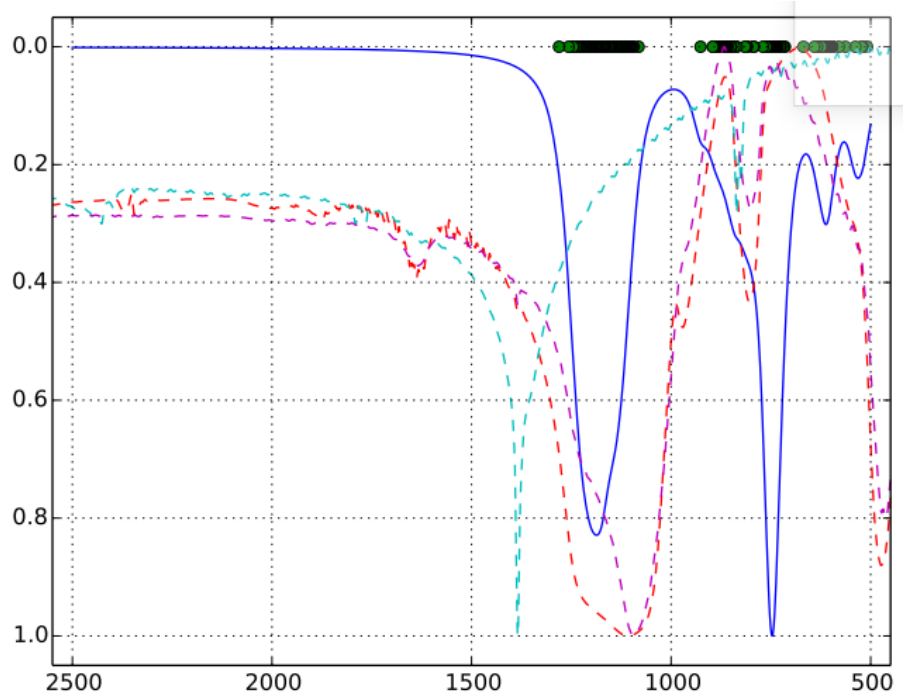

Figure 11. *IR spectrum nanofluid without chemical reaction.*

The following table shows the vibrational frequencies of the nanofluid without chemical reaction as well as the assignment of these frequencies:

Signal	Frequency (cm^{-1})	Assignment
A	1415	N-O stretching
B	1389	N-O stretching
C	1235	Si-O and N-O stretching
D	1188	Si-O and N-O stretching
E	1112	Si-O and N-O stretching
F	926	Si-OH stretching
G	748	N out-of-plane bending
H	538	Si-O-Si stretching

Table 7. *Frequencies nanofluid without chemical reaction.*

As we can observe the introduction of the silica cluster in the solar salt modifies the frequencies and the bands suffer a displacement. Thus, we find a displacement of the bands of the Si-O-Si stretching (C, D and E signals), that are now over 1230-1000 cm^{-1}.

In the following figure are shown the vectors of movement for the vibrations of silica cluster inside the solar salt:

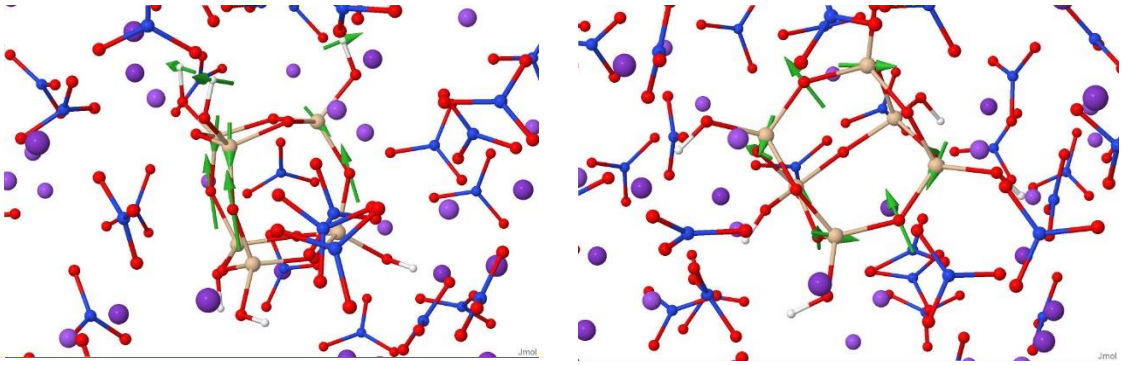

Figure 12. *Vectors of movement of Si-OH and Si-O-Si stretching respectively.*

In the second model of nanofluid a nitrate group is introduced in the silica cluster. The possible mechanism of this reaction will be discussed in the following section. ***Figure 13*** shows the model of nanofluid with chemical reaction:

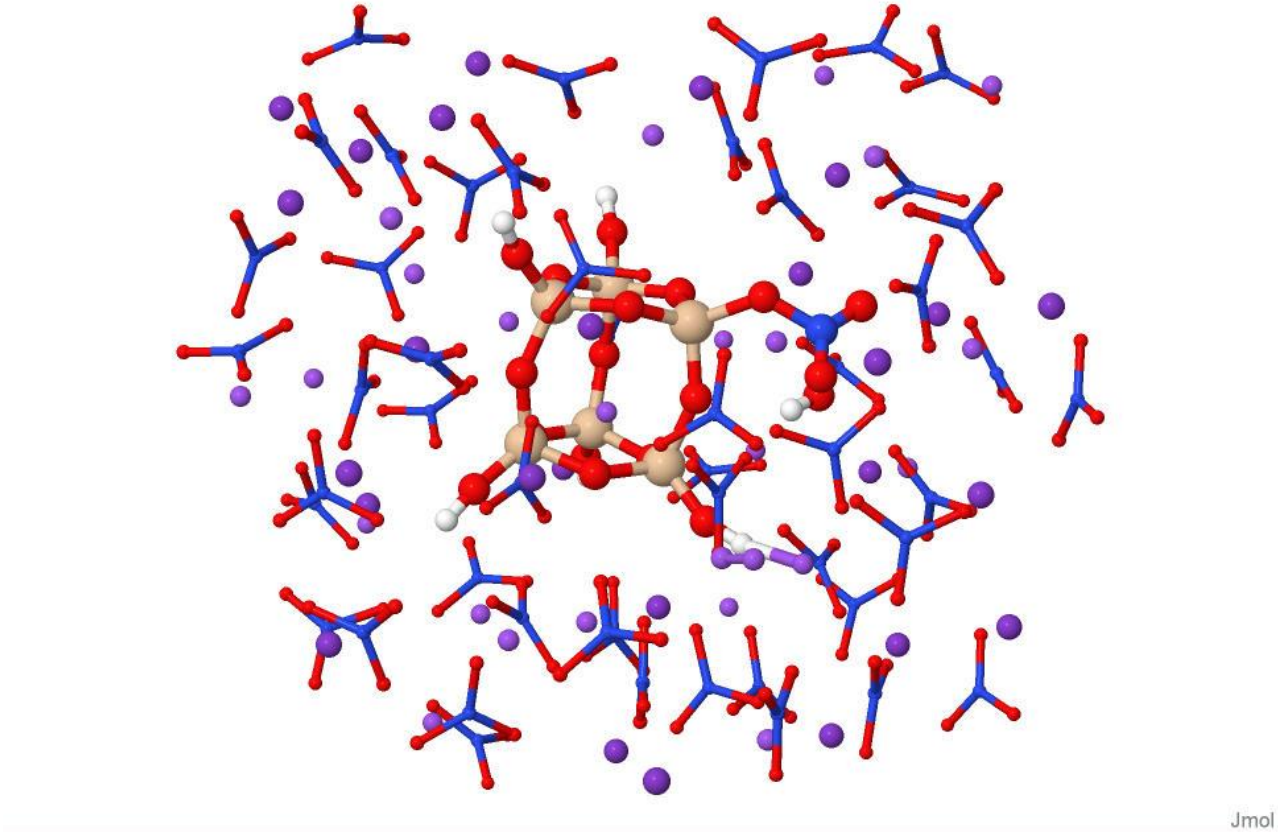

Figure 13. *Solar salt silica cluster interaction with chemical reaction.*

The theoretical IR spectrum (blue line) is represented together with the three experimental spectra of nanofluid (red dotted line) as is shown in ***Figure 14***:

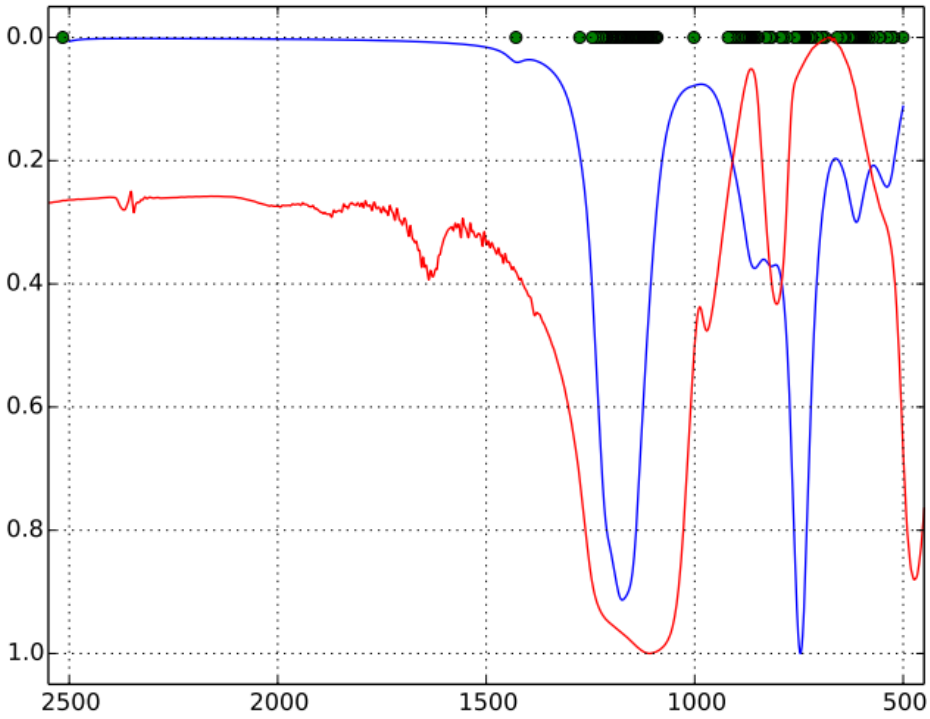

Figure 14. *IR spectrum nanofluid with chemical reaction.*

The following table shows the vibrational frequencies of the nanofluid with chemical reaction as well as the assignment of these frequencies:

Signal	Frequency (cm^{-1})	Assignment
A	1428	O_2N-O-Si stretching
B	1152	Si-O-Si and N-O stretching
C	862	Si-OH stretching
D	847	Si-OH stretching
E	744	N out-of-plane bending
F	610	N-O stretching
G	538	Si-O-Si stretching

Table 8. *Frequencies nanofluid with chemical reaction.*

With the introduction of a nitrate group in the silica cluster a new frequency appears at 1428 cm^{-1} (signal A). This frequency corresponds only to the vibration of the nitrate group attached to the silicon in the nanoparticle. This is a great evidence that allows us to check if the introduction of a nitrate group is possible or not. In the experimental spectrum, small bands with a lot of noise are observed, so it is difficult to know if it is the same band. The Si-O-Si (signal B) band has widened due to the nitrates of solar salt which overlap at the same frequency.

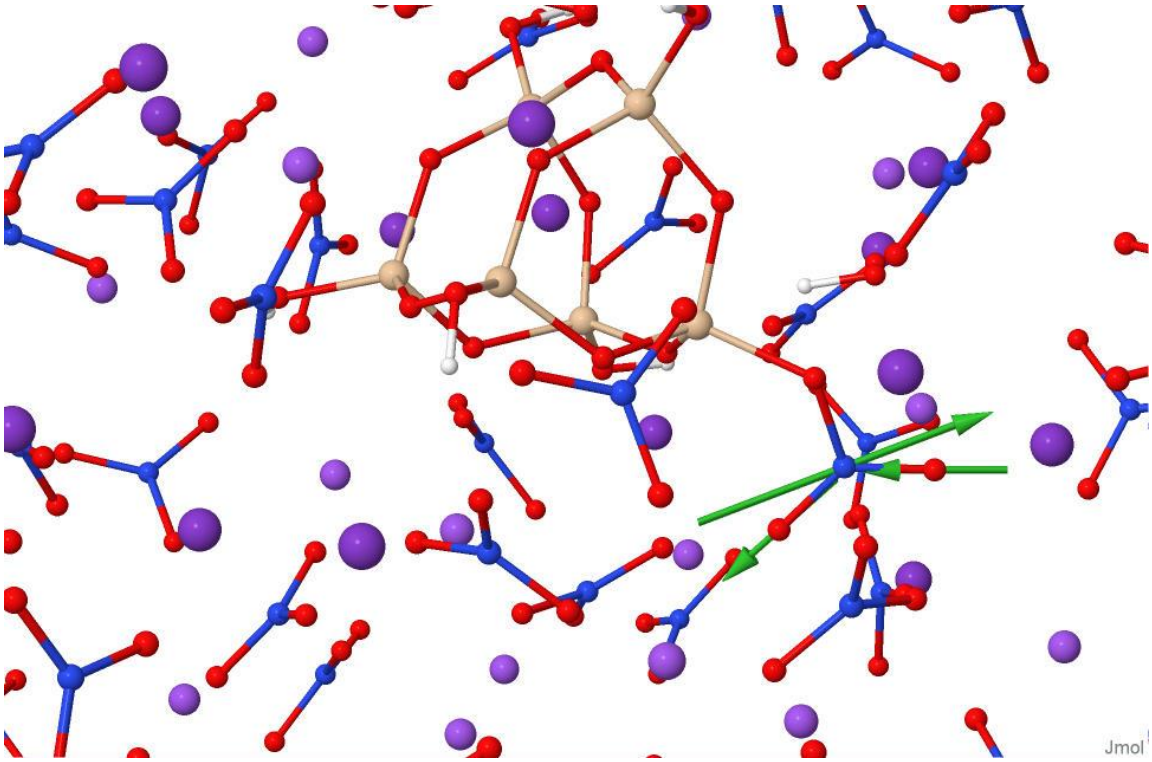

Figure 15. *Vector of movement for the vibration of the introduced nitrate.*

4.3 Chemical reaction

Once we have analysed the IR spectra, we must study the introduction of the nitrate group into the silica cluster. For this purpose, we will make a thermodynamic study as we have already done with the silica clusters, where we will obtain both the Gibbs-free energy and the equilibrium constant to check if the reaction is exothermic and therefore, if a nitrate group is introduced.

In order to make the calculations we have selected the cluster of 8 silicon atoms to represent the silica nanoparticles. The reaction studied is as follows:

$$Si_8O_{12}(OH)_8 + 41\ NO_3^- \rightarrow Si_8O_{12}(NO_3)(OH)_7 + 40\ NO_3^- + OH^-$$

	Molecule	E_o+G_{corr} (kJ/mol)
Reagents	$Si_8O_{12}(OH)_8 + NO_3^-$	-96687662.82
Products	$Si_8O_{12}(NO_3)(OH)_7 + OH^-$	-96687700.77

Table 9. *Internal energies for the nanofluid product.*

Applying [33], [34] and [35] equation we obtain:

ΔG^{o} (kJ/mol)	K_{eq}
-37.95	$4.05x10^{6}$

Table 10. *Equilibrium constant of nanofluid.*

4.4 Heat capacity calculations

Calculations of the calorific capacities of the nanofluid have been made, both for the model without chemical reaction and for the model with chemical reaction, in order to estimate the effect of the reaction on the increase of the specific heat. The results are shown below:

$CV_{without\ reaction}$ = 5586.443 J/mol·K at 780 K.

$CV_{with\ reaction}$ = 5597.466 J/mol·K at 780 K.

ΔCV = $\frac{5597.466-5586.443}{5586.443} x100 = 0.2\%$

The specific heat increase obtained for 10 %wt in nanoparticles is 0.2 %, a value that is quite far from the experimental one (around 20 %).

5. CONCLUSIONS

This work has been useful for me to go deeper into a field of chemistry such as computational chemistry. In addition, I have been able to experience how a research work is carried out starting from scratch with only one experimental spectrum. I have learned to implement to my knowledge in chemistry programs like Gaussian09, which is a great tool for the study of chemical reactions and that has provided us with very valuable information to be able to carry out this work

It must be taken into account that in order to achieve the models used in this work, a great number of calculations have been made, discarding a large quantity of models that were not suitable to our study. The models used are the most representative within our calculation conditions and the programs used, as well as the objective of this TFG. We have added a last section as an appendix where calculations for smaller models are shown.

Analyzing the results, it is feasible to introduce a nitrate group in the silica nanoparticles, although it does not have a very high K_{eq}, it is an exergonic reaction and therefore the nitrate could be chemically absorbed to the surface of the nanoparticles.

In this work we have used 10% wt of nanoparticles obtaining an increase of the calorific capacity of 0.2%, a result that differs from the one obtained experimentally with an increase of the specific heat of almost 20%. This is because we have not been able to reproduce the system necessary to obtain these results, using 1-2 %wt of nanoparticles. To reproduce such a system would have been very costly in terms of calculation and

would not have been feasible. On the other hand, a plausible reason for the small increase of heat capacity measured expeirmentally at 10 %wt of nanoparticles can be due to the presence of agglomeration, leading to a decrease in the available specifc surface, thus causing that fewer nitrate groups are combined with the nanoparticles. To improve the study, additional factors and computational techniques, beyond the scope of this TFG, should be taken into account.

6. APPENDIX

In this appendix we have decided to compile all those small models that have helped to reach the results of this work. Calculations were made with less computational cost and the results were analysed, from there, new models were discarded or implemented in order to obtain the definitive ones.

In order to study the behaviour of silica clustering and to achieve the final model of the 8-silicon cluster, we analysed smaller models with less silicon atoms.

A total of three models have been studied before arriving at the model used in this research. These models were formed from 2, 3, and 4 silicon atoms.

- Reaction 2 silicon atoms

$$\mathbf{2\ Si(OH)_4 \leftrightarrow Si_2O(OH)_6 + H_2O}$$

Nº Molecules	Molecule	E_o+Gcorr (Ha)
2	$Si(OH)_4$	-1185.76578
1	$Si_2O(OH)_6$	-1185.834873
1	H_2O	

Table 11. *Internal energies for the clustering of 2 silicon atoms (Ha).*

Applying [33], [34] and [35] equation we obtain:

ΔG^{o} (kJ/mol)	K_{eq}
-181.403672	$3.86x10^{31}$

Table 12. *Equilibrium constant of 2 silicon model.*

- Reaction 3 silicon atoms

$$\mathbf{3\ Si(OH)_4 \leftrightarrow Si_3O_3(OH)_6 + 3\ H_2O}$$

Nº Molecules	Molecule	E_o+Gcorr (Ha)
3	$Si(OH)_4$	-1778.64867
1	$Si_3O_3(OH)_6$	-1778.730151
3	H_2O	

Table 13. *Internal energies for the clustering of 3 silicon atoms (Ha).*

Applying [33], [34] and [35] equation we obtain:

ΔG^o (kJ/mol)	K_{eq}
-213.928365	$1.78x10^{37}$

Table 14. *Equilibrium constant of 3 silicon model.*

- Reaction 4 silicon atoms

$$\mathbf{4\ Si(OH)_4 \leftrightarrow Si_4O_4(OH)_8 + 4\ H_2O}$$

Nº Molecules	Molecule	E_o+Gcorr (Ha)
4	$Si(OH)_4$	-2371.53156
1	$Si_4O_4(OH)_8$	-2371.647111
4	H_2O	

Table 15. *Internal energies for the clustering of 4 silicon atoms (Ha).*

Applying [33], [34] and [35] equation we obtain:

ΔG^o (kJ/mol)	K_{eq}
-303.37915	$6.68x10^{52}$

Table 16. *Equilibrium constant of 4 silicon model.*

For these three designs, we have calculated the internal energy of the water molecules separately from the silica cluster as opposed to the work, where the water molecules are in the same model along with the silica cluster. Thus, the results obtained only give us qualitative information about the formation of the clusters, being in all cases an exergonic reaction.